

**HIGH FIGURE OF MERIT (FOM) VERSATILE 5G
C BAND NEW RADIO IQ RECEIVER SYSTEM**

PRAVINAH NAIR A/P SHASIDHARAN

UNIVERSITI SAINS MALAYSIA

2025

**HIGH FIGURE OF MERIT (FOM) VERSATILE 5G
C BAND NEW RADIO IQ RECEIVER SYSTEM**

by

PRAVINAH NAIR A/P SHASIDHARAN

**Thesis submitted in fulfilment of the requirements
for the degree of
Doctor of Philosophy**

April 2025

ACKNOWLEDGEMENT

Albert Einstein's assertion that "imagination is more important than knowledge" and his encouragement to "learn from yesterday, live for today, hope for tomorrow" have profoundly inspired me. These words fueled my passion for innovation, driving me to complete my thesis with great enthusiasm. I express deep gratitude to my supervisor, Assoc Prof. Dr. Jagadheswaran Rajendran, for his inspiring guidance and mentorship. His humility and enthusiasm for sharing ideas, ensuring no obstacles during my research project. I also acknowledge the financial assistance from the Crest Industry Graduate Research Assistant Scholarship Program (CREST-i-GRASP), which was pivotal throughout my project. The collaboration with companies like Silterra Malaysia Sdn Bhd, Intel, TSMC, and ST Microelectronics provided technical knowledge and support during the measurement process. I extend my gratitude to my PhD colleagues and friends for their support. Special thanks go to senior research officers Puan Sofiyah and Puan Nuha for their assistance during my PhD journey. I express my heartfelt gratitude to my parents, especially my late father, Mr. Shasidharan Chundu Nair, and my mother, Ms. Mageswari Perumal, for their love, prayers and encouragement. I also thank my uncle, Mr. Moses Raj, aunty Annie Mosses, Pastor Michelle John for their prayers ensuring me to have a smooth process throughout my studies. I truly appreciate the support from Sukyo Mahikari members and Intel member Lee Seng Siong, who guided and motivates me to think creatively and solve problems was invaluable. Lastly, endless thanks to great God for His blessing, guidance, divine protection and providing opportunities and making impossible things for me possible. I would like to thank everyone who have contributed to my thesis and push me to ensure my thesis completed gracefully.

TABLE OF CONTENTS

ACKNOWLEDGEMENT	ii
TABLE OF CONTENTS	iii
LIST OF TABLES	ix
LIST OF FIGURES	ix
LIST OF SYMBOLS	xxiii
LIST OF ABBREVIATIONS	xxv
LIST OF APPENDICES	xxix
ABSTRAK	xxx
ABSTRACT	xxxi
CHAPTER 1 INTRODUCTION	1
1.1 Research Background.....	1
1.1.1 Introduction	1
1.2 Receiver for 5G Applications.....	4
1.3 Receiver for 5G C Band applications and design specs.....	4
1.3.1 The challenges in Meeting 5G C Band	5
1.3.2 The challenges in 5G Band, which narrows towards Sub 6 GHz New Radio GHz	7
1.3.2(a) The advantages of Sub 6 GHz	8
1.3.2(b) The approach towards Sub 6 GHz	10
1.3.3 Low Power Receiver	13
1.4 Challenges and Trade-Offs in the Sub 6 GHz Receiver system	15
1.5 Problem Statement	16
1.6 Research Objectives	19
1.7 Thesis Scope	20
1.8 Thesis Organization	22

CHAPTER 2	LITERATURE REVIEW	23
2.1	Introduction	23
2.2	LNA Overview	24
2.2.1	LNA Performance Parameters	24
2.2.1(a)	LNA Gain.	25
2.2.1(b)	LNA S-Parameter.	25
2.2.1(c)	LNA Stability.....	30
2.2.1(d)	LNA Noise Figure, NF.	31
2.2.1(e)	LNA Linearity, IIP3.....	32
2.2.2	LNA Topologies.....	37
2.2.3	Summary	47
2.3	Mixer Overview	52
2.3.1	Mixer Performance Parameters	52
2.3.1(a)	Mixer Conversion Gain.	52
2.3.1(b)	Mixer S-Parameter.....	54
2.3.1(c)	Mixer Linearity.....	56
2.3.1(d)	Mixer Noise Figure, NF.....	63
2.3.1(e)	Mixer Port Isolation.....	66
2.3.2	Mixer Topologies	68
2.3.3	Mixer Techniques and its challenging Trade-Offs.....	78
2.3.4	Summary	91
2.4	VCO Overview	94
2.4.1	VCO Performance Parameters	94
2.4.1(a)	Phase Noise	96
2.4.1(b)	Start-up	100
2.4.1(c)	Output Power	103
2.4.1(d)	Power Consumption	103

2.4.2	VCO Classes	104
2.4.2(a)	Class B VCO	104
2.4.2(b)	Class C VCO	107
2.4.2(c)	Class AB	109
2.4.2(d)	Class D	112
2.4.2(e)	Class F ₃ ,F ₂ ,F _{2,3}	113
2.4.3	VCO Topologies	117
2.4.4	Summary	132
2.5	Receiver Overview	135
2.5.1	Receivers Sub 6 GHz receiver works.....	136
2.5.2	Summary	152
CHAPTER 3 METHODOLOGY.....		153
3.1	Introduction	153
3.2	Design Specification	157
3.3	The Development of the Wideband LNA	162
3.3.1	Inductive Source Degenerated Cascoded (ISDC) Design and Analysis for Gain, Noise and Bandwidth Enhancement.....	168
3.4	The Development High Linearity, Wideband and High Isolation Quadrature I and Q Generation with Mixer and Transimpedance Amplifier (TIA)	175
3.5	The Development Hybrid VCO for Wideband and High FOM and Low PN	206
3.5.1	Wideband Hybrid VCO.....	208
3.6	Receiver Layout Implementation	218
3.7	Estimation of the Receiver FoM	221
3.8	Simulation and Measurement Test Setup	224
3.8.1	LNA testbench setup	224
3.8.2	IQ mixer testbench setup.....	224
3.8.3	VCO testbench setup.....	225

3.8.4	Receiver measurement testbench setup.....	226
3.9	Summary	238
CHAPTER 4 RESULTS AND DISCUSSION.....		239
4.1	Introduction	239
4.2	Characterization for Receiver Specification from pre-schematic simulation to post-layout verification	239
4.3	LNA, Mixer ,VCO and Entire Receiver Result	240
4.3.1	LNA Schematic Results	240
4.3.1(a)	S parameters	240
4.3.1(b)	LNA Stability and Noise Figure	242
4.3.1(c)	LNA Linearity,IIP3	243
4.3.1(d)	LNA Linearity,IIP3 Vs V_{DD}	245
4.3.1(e)	Noise Figure,NF Vs V_{DD}	246
4.3.2	LNA Post Layout Results.....	252
4.3.2(a)	LNA S parameters	252
4.3.2(b)	LNA Stability and Noise Figure	253
4.3.2(c)	LNA Linearity,IIP3	255
4.3.3	IQ Down Conversion Mixer Schematic Results	261
4.3.3(a)	S parameters	262
4.3.3(b)	Voltage Conversion Gain (VCG)	263
4.3.3(c)	Power Conversion Gain (PCG)	265
4.3.3(d)	Output Power	266
4.3.3(e)	Intermodulation and Intercept Points	267
4.3.3(f)	Port to Port Analysis	272
4.3.3(g)	DC offset Voltage across LO Power	273
4.3.3(h)	Noise Figure Analysis.....	275
4.3.4	IQ Down Conversion Mixer Post Layout Simulation Results	276
4.3.4(a)	S parameters	276

4.3.4(b)	Voltage Conversion Gain (VCG)	277
4.3.4(c)	Power Conversion Gain (PCG)	278
4.3.4(d)	Output Power	279
4.3.4(e)	Intermodulation Distortion and Intercept Points	280
4.3.4(f)	Port to Port Analysis	284
4.3.4(g)	P1dB Compression Point.....	285
4.3.4(h)	Noise Figure.....	286
4.3.5	Voltage Controlled Oscillator (VCO) Pre Layout Results.....	287
4.3.6	Voltage Controlled Oscillator (VCO) Post Layout Results	302
4.3.7	Receiver Post Layout Result	310
4.3.7(a)	S parameters	310
4.3.7(b)	Gain and Noise Figure	311
4.3.7(c)	Transient Signal Results	312
4.3.7(d)	VCO Phase Noise	315
4.3.7(e)	IF Quadrature outputs	316
4.3.7(f)	IF Intermodulation Distortion and Linearity	320
4.3.7(g)	IF Power Gain across RF Input Power	323
4.3.7(h)	IF Voltage Gain across LO Input Power	324
4.3.7(i)	IF Output Power across RF Input Power.....	325
4.3.8	Receiver Measurement Results	326
4.3.8(a)	Measured S parameters	326
4.3.8(b)	Measured Port to Port Isolation	327
4.3.8(c)	Measured IF Conversion Gain Vs VCO Input Power	328
4.3.8(d)	Measured IF Output Power Vs RF Input Power.....	330
4.3.8(e)	Measured IF Linearity, IIP3	331
4.3.8(f)	Measured IF Noise Figure	331
4.3.8(g)	Measured VCO Start-up	332

4.3.8(h)	Measured VCO Phase Noise	334
4.3.8(i)	Measured VCO Eye Margin	338
4.3.8(j)	Measured Transient output of IF	339
4.3.11	Receiver Summary	343
CHAPTER 5 CONCLUSION AND FUTURE RECOMMENDATIONS....		349
5.1	Conclusion.....	349
5.2	Recommendations for Future Research	350
REFERENCES.....		352
APPENDICES		
LIST OF PUBLICATIONS		

LIST OF TABLES

		Page
Table 2.1	Performance Comparison of LNA Research Work	51
Table 2.2	Performance Comparison of Mixer Research Work	93
Table 2.3	Overall efficiency of the VCO classes	116
Table 2.4	VCO Recent Work Comparison.....	134
Table 2.5	Performance Comparison of Receiver Research Work	152
Table 3.1	Target Specification of full Sub 6 GHz Receiver System [1],[2],[24],[228],[231]	161
Table 3.2	LNA components values used in the design	163
Table 3.3	IQ Generation circuit, Mixer and TIA components values used in the design	179
Table 3.4	VCO components values used in the design	209
Table 4.1	Quadrature IF amplitude imbalance and phase error	318
Table 4.2	LNA standalone schematic and post layout of S parameter results .	343
Table 4.3	LNA standalone schematic and post layout of Noise Figure, NF result.....	343
Table 4.4	LNA standalone schematic and post layout, IIP3 result	344
Table 4.5	IQ standalone mixer S parameter schematic and post layout result.	344
Table 4.6	IQ IF Conversion Gain schematic and post layout results.....	344
Table 4.7	IQ IF IIP3, Port to Port Isolation and Noise schematic and post layout result.....	344
Table 4.8	Hybrid VCO schematic and post layout result.....	345
Table 4.9	Performance summary of the proposed receiver circuit.	346
Table 4.10	Performance comparison of the receiver with other reported works.	347

LIST OF FIGURES

		Page
Figure 1.1	5G Interconnected network [1]	1
Figure 1.2	5G cases landscape[3]	2
Figure 1.3	Sub 6 GHz NR Receiver for C Band range [14]	6
Figure 1.4	The feature towards enhancing sub 6 GHz [16]	11
Figure 1.5	Network Spectrum Bands of 5G	12
Figure 2.1	S-Parameter Representation of Two-Port Network [47]	26
Figure 2.2	Common source inductive degeneration topology[51].....	28
Figure 2.3	Small signal equivalent model	28
Figure 2.4	The Equivalent Model for Noise Figure of Cascaded Components.	32
Figure 2.5	1-dB compression point [58]	33
Figure 2.6	Input Third order intercept point [58].	34
Figure 2.7	The IMD components induced by a nonlinear device [59]	36
Figure 2.8	Modified Cascode LNA with IMD linearizer [64]	37
Figure 2.9	Wideband LNA using CG and CS stage [68]	38
Figure 2.10	Wideband Variable Gain LNA [69]	39
Figure 2.11	(a) Predistortion (b) Post-distortion linearisation technique [72]	41
Figure 2.12	Single stage CG LNA with negative feedback[79]	42
Figure 2.13	Inductorless Wideband LNA with Gm ehancement [83]	43
Figure 2.14	Broadband noise matching and ultra-low noise LNA [86]	44
Figure 2.15	Triple-Path Noise Cancelling wideband LNA [89]	45
Figure 2.16	Noise- cancelling LNA with active feedforward [90]	46
Figure 2.17	5G LNA noise reduction and current reuse technique [91]	47

Figure 2.18	The FoM and the percentage of power consumption of the LNA research work	48
Figure 2.19	The Gain, Linearity and NF comparison of the LNA works	50
Figure 2.20	S-Parameter representation of three port network	54
Figure 2.21	Illustration of 1 dB compression point response [95]	57
Figure 2.22	Frequency spectrum of the IIP3 measurement [96]	60
Figure 2.23	Graphical representation of IIP3 and OIP3 [96]	61
Figure 2.24	Noise in the amplification of a system [95] - [97]	63
Figure 2.25	Graphical interpretation of noise factor [95] - [102]	64
Figure 2.26	Noise in the Ideal mixer [97]	65
Figure 2.27	Double balanced switching passive mixer [104] - [105].	69
Figure 2.28	Unbalanced switching passive mixer [104] - [105]	70
Figure 2.29	Single Balanced Mixer (a) circuit (b) conceptual equivalent circuit [102] - [105]	71
Figure 2.30	Schematic of double balanced mixer [108]	74
Figure 2.31	Current Bleeding Double balance Gilbert Cell Mixer[109]	79
Figure 2.32	Double balance mixer with current reuse technique [110]	80
Figure 2.33	Conventional double balanced Gilbert cell mixer with folded technique [63].....	81
Figure 2.34	The proposed Dynamic current injection mixer[119]	82
Figure 2.35	The self-biased mixer [120]	83
Figure 2.36	Linear Bulk Injection Mixer [121]	84
Figure 2.37	Proposed Mixer First receiver [125]	85
Figure 2.38	Full Duplex Mixer First Receiver [126]	86
Figure 2.39	Parallel Sliding IF Receiver Front End [127]	87
Figure 2.40	Direct Conversion Receiver for Multicarrier 3G/4G [129]	88
Figure 2.41	Sub Harmonic IQ Receiver [130][137].....	90

Figure 2.42	Symmetrical RC polyphase filter used to generate I and Q [130][137]	90
Figure 2.43	FoM of the mixer with its corresponding percentage of power consumption	92
Figure 2.44	The Gain, Linearity and NF comparison of the mixer works.	92
Figure 2.45	Phase noise region for open loop and closed loop oscillator against frequency offset [144]	95
Figure 2.46	(a) An ideal LC tank with a current impulse; phase response when the current impulse is injected at (b) the peak voltage and (c) zero crossing point [146]-[147]	97
Figure 2.47	AM-to-PM conversion of the current-biased oscillator [149]-[152]	98
Figure 2.48	Effect of the AM on the average capacitance of varactor containing (a) odd-order terms (left) and (b) even-order terms(right)[149]-[152]	99
Figure 2.49	Path of the tank current harmonics I_{H1} , I_{H2} and I_{H3} [153]-[154]	100
Figure 2.50	The schematics of UWB VCO [155]	101
Figure 2.51	Start up transient of VCO for different value of (W/L) mismatch[155].....	102
Figure 2.52	Comparison between (a) ideal and (b) real class-B oscillator[160]-[161]	105
Figure 2.53	Class-D oscillator and its output waveform[162]	106
Figure 2.54	Class-C oscillator and its corresponding voltage and current waveform [165].....	107
Figure 2.55	Hybrid class-B/class-C oscillator [166]	109
Figure 2.56	Dynamic bias class-C oscillator employing op-amp and RC filter [168]	109
Figure 2.57	Schematic of hybrid class-AB/class B VCO[169]	110

Figure 2.58	Start-up simulation a) class AB VCO b) hybrid class AB and class B VCO.[169]	111
Figure 2.59	Class-D oscillator and its output waveform [164]	112
Figure 2.60	Class-F3 oscillator [173].....	114
Figure 2.61	Class-F3 oscillator, its corresponding voltage and ISF waveform [173]	114
Figure 2.62	Class-F2 oscillator, its corresponding voltage and ISF waveform [172]-[173]	115
Figure 2.63	Schematic of a dual type conduction CMOS Class C-VCO [175]	118
Figure 2.64	Measured phase noise at 4.5 GHz oscillation frequency [175].....	118
Figure 2.65	Resistor added dual-conduction class-C VCO.[176]	119
Figure 2.66	Measurement result of the phase noise [176].	120
Figure 2.67	Reconfigurable dual core VCO [177]	120
Figure 2.68	Hybrid class B/class-C oscillator.[166]	122
Figure 2.69	Phase noise measurements at mid band for $V_{bias1} = 1.2V$ (class B mode) and $V_{bias1} 0.5 V$ (Class-C mode) [166].....	123
Figure 2.70	Class-C (a) with dynamic bias (b) hybrid Class-B /Class-C Oscillator [182]	123
Figure 2.71	Class-F _{2,3} Oscillator [171]	124
Figure 2.72	Traditotional Voltage Biased Oscillator [172]	125
Figure 2.73	Preliminary class F-1 oscillator with single ended output [174]	126
Figure 2.74	28nm CMOS technology LC VCO [184]	127
Figure 2.75	The schematic of the proposed dual digital feedback loops [188]..	129
Figure 2.76	CMOS VCO with Tail Current Source Feedback [39]	130
Figure 2.77	High swing Class-C VCO with current control feedback [196] ...	131
Figure 2.78	VCO related works comparison illustrated in percentage of a) Power consumption b) Figure of Merit	132

Figure 2.79	Phase Noise, (PN) and Tuning Range (TR) comparison of the VCO research works	133
Figure 2.80	RF Bluetooth receiver architecture [207]	136
Figure 2.81	Block diagram of power receiver.[209]	137
Figure 2.82	CMOS MedRadio Receiver [212]	138
Figure 2.83	The LMV Cell topology [218]	139
Figure 2.84	Phase and thermal noise cancelling receiver [220]	141
Figure 2.85	Mixer First Receiver with Class F Adiabatic Switching [225]	142
Figure 2.86	Diagram of Harmonic Recombination Receiver[226]	143
Figure 2.87	Dual Band Tunable Gain Sub Sampling Receiver [24]	144
Figure 2.88	Highly linear I channel Receiver.[228]	145
Figure 2.89	Full duplex Receiver with Self Interference cancelation [229]	146
Figure 2.90	Mixer first Receiver using baseband reactance cancelling LNA [230]	147
Figure 2.91	Wideband Receiver architecture [231]	148
Figure 2.92	Multibeam MIMO receiver [17]	149
Figure 2.93	FoM Receiver work architecture.	150
Figure 2.94	Receiver work with comparison of gain, linearity and NF.	151
Figure 3.1	The flow chart of the design methodology.	156
Figure 3.2	The Block Diagram of the receiver design	158
Figure 3.3	Entire proposed 5G C Band New Radio IQ Receiver System	159
Figure 3.4	Wideband LNA Schematic	162
Figure 3.5	A typical CMOS bias circuit	164
Figure 3.6	The illustration of the modified bias circuit	165
Figure 3.7	APD Amplifier stage a) Triple cascode stage configuration b) Small signal equivalent circuits.	166

Figure 3.8	(a) CS inductive source degenerated cascode LNA (b) Small signal model of the CS inductive source degenerated cascode.	169
Figure 3.9	Small signal model of the input of the inductive degenerated common source amplifier	172
Figure 3.10	Equivalent circuit for input stage noise calculations for an inductively degenerated LNA.	173
Figure 3.11	Current reuse concept for the RF Front End	175
Figure 3.12	Proposed concept of the receiver	177
Figure 3.13	The overall proposed LNA IQ generation circuit with IQ mixer and TIA	178
Figure 3.14	The I and Q generation circuit for the LNA	182
Figure 3.15	The traditional poly phase RC filter for IQ generation	183
Figure 3.16	The minimum sideband signal for the IIP3.....	191
Figure 3.17	The worst case sideband signal for the IIP3.....	191
Figure 3.18	The sideband signal for the IIP2	192
Figure 3.19	The port-to-port isolation analysis for half circuit for I phase	193
Figure 3.20	Single Balanced Mixer	195
Figure 3.21	Proposed mixer architecture	195
Figure 3.22	A sine wave of two phases VLO injected to the mixer	197
Figure 3.23	Proposed VCO architecture	208
Figure 3.24	(a) SQB structure (b) Small signal of SQB	210
Figure 3.25	The Q factor comparison with the conventional VCO and the proposed architecture.	213
Figure 3.26	Schematic of the TVCO	213
Figure 3.27	Small signal model of the TVCO	214
Figure 3.28	Simplified model of the TVCO	216
Figure 3.29	Small signal of the 1/f noise model of the TVCO	216

Figure 3.30	The physical layout of wideband Sub 6 GHz Receiver including the RFESD Pads (core area only:1.3mm ²).	220
Figure 3.31	The Testbench setup for the Schematic and Post layout simulation of the LNA	224
Figure 3.32	The test bench setup for schematic and post layout simulations for the IQ downconversion mixer	225
Figure 3.33	The test bench setup for schematic and post layout simulations for the proposed Hybrid VCO	226
Figure 3.34	Photomicrograph of the fabricated chip	227
Figure 3.35	Summit 9000 probe station with measurement equipment set up. .	228
Figure 3.36	RF probe and DC probe testing on the proposed receiver system.	228
Figure 3.37	Summit 9000 probe station from Cascade Microtech.	229
Figure 3.38	Test setup for measuring S parameter of the proposed Sub 6 GHz receiver.	231
Figure 3.39	Test setup for RF-to-IF isolation measurement	232
Figure 3.40	Test setup for conversion gain	233
Figure 3.41	Test setup for IIP3 measurement	235
Figure 3.42	Calibration of noise figure measurement	236
Figure 3.43	Test setup for noise figure measurement of the proposed circuit.	237
Figure 4.1	The S parameter of the post layout simulation of the Standalone LNA	241
Figure 4.2	The Stability, Kf and noise figure (NF) of the LNA	242
Figure 4.3	The IIP3 of LNA at 3 GHz	244
Figure 4.4	The IIP3 of LNA at 4 GHz	244
Figure 4.5	The IIP3 of LNA at 5 GHz	245
Figure 4.6	The IIP3 of LNA Vs V _{DD}	246
Figure 4.7	The NF of LNA Vs V _{DD}	247
Figure 4.8	Monte Carlo Simulations of the Proposed LNA's NF at 3 GHz	248

Figure 4.9	Monte Carlo Simulations of the Proposed LNA's NF at 4 GHz	249
Figure 4.10	Monte Carlo Simulations of the Proposed LNA's NF at 5 GHz	249
Figure 4.11	The Gain of LNA Vs V_{DD}	250
Figure 4.12	Monte Carlo Simulations of the Proposed LNA's Gain at 3 GHz .	251
Figure 4.13	Monte Carlo Simulations of the Proposed LNA's Gain at 4 GHz .	251
Figure 4.14	Monte Carlo Simulations of the Proposed LNA's Gain at 5 GHz .	252
Figure 4.15	The S parameter of the post layout simulation of the Standalone LNA	253
Figure 4.16	The post simulation of the Stability, Kf and noise figure (NF) of the LNA	254
Figure 4.17	The post simulation of the LNA IIP3 at 3 GHz	256
Figure 4.18	The post simulation of the LNA IIP3 at 4 GHz	256
Figure 4.19	The post simulation of the LNA IIP3 at 5 GHz	257
Figure 4.20	Monte Carlo Post Simulations of the Proposed LNA's NF at 3 GHz	258
Figure 4.21	Monte Carlo Post Simulations of the Proposed LNA's NF at 4 GHz	258
Figure 4.22	Monte Carlo Post Simulations of the Proposed LNA's NF at 5 GHz	259
Figure 4.23	Monte Carlo Post Simulations of the Proposed LNA's gain, S21 at 3 GHz	260
Figure 4.24	Monte Carlo Post Simulations of the Proposed LNA's gain, S21 at 4 GHz	260
Figure 4.25	Monte Carlo Post Simulations of the Proposed LNA's gain, S21 at 5 GHz	261
Figure 4.26	The S Parameter of the IQ Down conversion mixer	262
Figure 4.27	The voltage conversion gain of IF frequency across to its frequency	263

Figure 4.28	The voltage conversion gain of IF frequency across the RF LNA input power.	264
Figure 4.29	The power conversion gain of the IF under RF condition of 3,4 and 5 GHz respectively.	265
Figure 4.30	The output power of the IF under RF condition of 3,4 and 5 GHz respectively.	267
Figure 4.31	The IIP3 of mixer at 3 GHz	268
Figure 4.32	The IIP3 of the mixer at 4 GHz	269
Figure 4.33	The IIP3 of the mixer at 5 GHz	269
Figure 4.34	The Monte Carlo simulation of IIP3 of the mixer at 3 GHz	270
Figure 4.35	The Monte Carlo simulation of IIP3 of the mixer at 4 GHz	271
Figure 4.36	The Monte Carlo simulation of IIP3 of the mixer at 5 GHz	271
Figure 4.37	Simulated port to port isolation of the signal.	273
Figure 4.38	DC offset voltage from the LO self-mixing versus LO power simulated for the proposed IQ mixer and conventional mixer.	274
Figure 4.39	1 dB Compression point of the IQ mixer	275
Figure 4.40	The Noise Figure of the Standalone Mixer	276
Figure 4.41	The post layout simulation of the S parameter of the Standalone Mixer	277
Figure 4.42	The post layout simulations of the VCG of the standalone mixer ..	278
Figure 4.43	The post layout simulations of the PCG of the standalone mixer ..	279
Figure 4.44	The output power of the IF under RF condition of 3,4 and 5 GHz respectively.	280
Figure 4.45	The post layout simulation of IIP3 of the mixer at 3 GHz	281
Figure 4.46	The post layout simulation of IIP3 of the mixer at 4 GHz	281
Figure 4.47	The post layout simulation of IIP3 of the mixer at 5 GHz	282
Figure 4.48	The post layout Monte Carlo simulation of IIP3 of the mixer at 3 GHz	283

Figure 4.49	The post layout Monte Carlo simulation of IIP3 of the mixer at 4 GHz	283
Figure 4.50	The post layout Monte Carlo simulation of IIP3 of the mixer at 5 GHz	284
Figure 4.51	The port to port analysis of the IQ mixer	285
Figure 4.52	Post layout simulation of the P1 dB Compression point	286
Figure 4.53	Pre layout and post layout simulation of the Noise Figure of the Mixer	287
Figure 4.54	Differential oscillation of the VCO	288
Figure 4.55	Start-up of the VCO	289
Figure 4.56	Simulated drain current of the VCO	290
Figure 4.57	Critical Gm for startup of the VCO	291
Figure 4.58	V_{GS} and V_{DS} of the proposed oscillator	291
Figure 4.59	Comparison analysis of the amplitude imbalance of proposed hybrid VCO with Class C VCO.	292
Figure 4.60	Performance of the phase noise across the VCO bandwidth	294
Figure 4.61	Power and frequency of the proposed hybrid VCO across the tuning voltage, V_{TUNE}	295
Figure 4.62	The performance of the phase noise of the proposed VCO architecture	296
Figure 4.63	The performance of the phase noise across corner	298
Figure 4.64	The performance of the output power of the proposed VCO architecture across corner	298
Figure 4.65	The performance of the phase noise of the proposed VCO architecture under 1MHz, 3 MHz and 10 MHz offset	299
Figure 4.66	The performance of the figure of merit of the proposed VCO architecture under 1MHz, 3MHz and 10MHz offset	300
Figure 4.67	The bias voltage, VG affect on the VCO frequency.	301

Figure 4.68	VCO start up in post layout performance.	302
Figure 4.69	Amplitude imbalance performance of the VCO in post layout simulation with comparison of pre layout simulation result.	303
Figure 4.70	Performance of the phase noise of the VCO across frequency.	304
Figure 4.71	Performance of the phase noise of the VCO at 1 MHz, 3 MHz and 10 MHz offset in post layout simulations.	305
Figure 4.72	Performance of the figure of merit (FoM) of the VCO at 1 MHz, 3 MHz and 10 MHz offset in post layout simulations.	306
Figure 4.73	Performance of the power and frequency across the tuning voltage.	307
Figure 4.74	Performance of the phase noise across corner	308
Figure 4.75	Performance of the power across in corner	309
Figure 4.76	The S parameter of the Receiver System	311
Figure 4.77	The Noise figure and Gain of the receiver system	312
Figure 4.78	The transient signal of the RF quadrature signals	313
Figure 4.79	The transient signal of the VCO output signals	314
Figure 4.80	The start-up of the VCO transient signal	315
Figure 4.81	The performance of the phase noise of the VCO in the integrated receiver system	316
Figure 4.82	Simulated gain mismatch of the quadrature IF output signal	317
Figure 4.83	Simulated phase shift of the quadrature IF output signal.....	318
Figure 4.84	Simulated post layout result of the quadrature I+ and Q- output signal	319
Figure 4.85	Simulated post layout result of the quadrature, I- and Q+ output signal	320
Figure 4.86	Post Layout performance of IIP3 of the IF under 3 GHz RF range	321

Figure 4.87	Post Layout performance of IIP3 of the IF under 4 GHz RF range	322
Figure 4.88	Post Layout performance of IIP3 of the IF under 5 GHz RF range	322
Figure 4.89	Performance of the IF power gain across LNA input power	323
Figure 4.90	Performance of the IF voltage gain across LO input power	324
Figure 4.91	Performance of the IF power gain across LO input power	325
Figure 4.92	Measured input and output reflection coefficient for RF and IF ports.	326
Figure 4.93	Measured results of RF-to -IF and IF-to-RF isolation	328
Figure 4.94	Measurement result of conversion gain versus LO input power according to the V_{TUNE} level.	329
Figure 4.95	Measurement result of 1dB compression point.	330
Figure 4.96	Test setup for IIP3 measurement	331
Figure 4.97	Noise figure of the receiver	332
Figure 4.98	Start-up measurement result of the integrated hybrid VCO	333
Figure 4.99	Phase Noise of the VCO at 3GHz range frequency under V_{DD} of 1.0 V	335
Figure 4.100	Phase Noise of the VCO at 4 GHz range frequency under V_{DD} of 1.0 V	336
Figure 4.101	Phase Noise of the VCO at 5 GHz range frequency under V_{DD} of 1.0 V	337
Figure 4.102	Eye Margin of the signal integrity of the VCO.....	338
Figure 4.103	Transient output of the IF	339
Figure 4.104	Transient output of the I and Q quadrature IF (increase per volts/div)	340
Figure 4.105	Transient output of the I and Q quadrature IF (decrease per volts/div)	341

Figure 4.106	Transient output of the I and Q quadrature IF (added external filter cap at In Phase Signal)	342
Figure 4.107	Transient output of the I and Q quadrature IF (added external filter cap at In Phase Signal and Quad Phase Signal)	342

LIST OF SYMBOLS

Φ	Conduction angle
γ	Channel thermal noise coefficient
ω	Frequency in rad/s
ω_C	Center Frequency in rad/s
ω_{IF}	IF angular frequency
\mathcal{L}	Leeson Phase noise
ξ	Riemann zeta function
ω_{LO}	LO angular frequency.
Ω	Ohm
$1/f$	Flicker Noise
C_{gs}	Gate-Source Parasitic Capacitance
C_{gd}	Gate-Drain Parasitic Capacitance
C_{ox}	Gate Oxide Capacitance
C_p	Parasitic Capacitance
f	Frequency in Hz
f_{IF}, ω_{IF}	Frequency of Intermediate Frequency Signal
f_{LO}, ω_{LO}	Frequency of Local Oscillator Signal
f_{RF}, ω_{RF}	Frequency of Radio Frequency Signal
f_t	Transit Frequency
g_m	Transconductance
k	Boltzmann's constant
NF_{LNA}	Noise figure of the LNA
L_g	Gate Inductor
L	Gate length of Transistor

P_{IF}	IF output power
P_{RF}	RF input power
P_{LO}	LO input power
r_o	Output resistance of the transistor
S	$j\omega$
T	Absolute Temperature
V_{DD}	Supply voltage
V_{TH}	Threshold Voltage of Transistor
W	Width of Transistor

LIST OF ABBREVIATIONS

4G	4 th Generation
5G	5 th Generation
AC	Alternating Current
AGC	Automatic Gain Control
AM	Amplitude Modulation
AM-AM	Amplitude Modulation to Amplitude Modulation
AM-PM	Amplitude Modulation to Phase Modulation
APD	Analogue Pre-Distorter
BC	Barkhausen Criterion
CCO	Current-controlled oscillator
CG	Common Gate
CG	Conversion Gain
CMO	Current- Mode Oscillator
CMOS	Complementary Metal Oxide Semiconductor
CS	Common Source
CSD	Capacitive Source Degeneration
CS	Capacitive Switching
DBM	Double Balanced Mixer
dB	Decibel
dBm	Decibel with respect to 1mW
DC	Direct Current
DM	Differential Mode
DRC	Design Rule Check
DSP	Digital Signal Processing
DUT	Device Under Test
EDA	Electronic Design Automation
F	Noise Factor
FS	Frequency Synthesizer
FM	Frequency Modulation
FRO	Free Running Oscillator
FT	Fourier Transform

GaAs	Gallium Arsenide
GBP	Gain Bandwidth Product
GC	Grounded -capacitor
GFSK	Gaussian Frequency Shift Keying
GPSK	Gaussian Phase Shift Keying
GND	Ground
GSGSG	Ground-Signal-Ground-Signal-Ground
GSO	Gate-Source Overdrive
HB	Harmonic Balance
HBAC	Harmonic Balance AC analysis
HO	Harmonic Oscillator
Hz	Hertz
IC	Integrated Circuit
IF	Intermediate Frequency
IM	Intermodulation
IMD3	3 rd Order Intermodulation Distortion
IMN	Input Matching Network
IoE	Internet of Everything
IoT	Internet of Things
IIP3	Input -referred Third-Order Intercept Point
IP3	Third -order Intercept Point
IQ	In-Phase, Quadrature-Phase
IR	Image Rejection
KCL	Kirchhoff's Current Law
KVL	Kirchhoff's Voltage Law
Kf	Stability
Kp	Process Parameter
LMV	LNA+Mixer+VCO
LNA	Low Noise Amplifier
LO	Local Oscillator
LP	Low Power
LTE	Long Term Evaluation
LVS	Layout Vs Schematic
MIM	Metal-Insulated-Metal

MOSFET	Metal-Oxide-Semiconductor Field-Effect Transistor
MC	Monte Carlo
NEF	Noise Excess Factor
NF	Noise Figure
NFA	Noise-Figure Analyzer
nMOS	N-Channel Mosfet
NR	New Radio
OIP3	Output-referred Third-Order Intercept Point
OMN	Output Matching Network
P1dB	1dB Compression Point
PM	Phase Modulation
pMOS	P-Channel Mosfet
PN	Phase Noise
PVT	Process, Voltage and Temperature
Qf	Quality Factor
QLNA	Quadrature Low Noise Amplifier
QVCO	Quadrature Voltage Controlled Oscillator
RF	Radio Frequency
RFIC	Radio Frequency Integrated Circuit
RMS	Root Mean Square
SBM	Single Balanced Mixer
S-Par	Scattering Parameter
SA	Spectrum Analyzer
SAW	Surface Acoustic Wave
Si	Silicon
SoC	System on Chip
SiGe	Silicon Germanium
SOI	Silicon on Insulator
SNR	Signal-To-Noise Ratio
SRF	Self – Resonance Frequency
SSA	Signal Source Analyzer
TIA	Trans-impedance Amplifier
UWB	Ultra-Wide Bandwidth
VCO	Voltage Controlled Oscillator

VG	Voltage Gain
VNA	Vector Network Analyzer
WPAN	Wireless Private Area Network

LIST OF APPENDICES

- Appendix A DERIVATIONS
Appendix B PUBLICATIONS

SISTEM PENERIMA PELBAGAI GUNA 5G JALUR FREKUENSI C IQ RADIO BAHARU DENGAN TAHAP MERIT (FOM) YANG TINGGI

ABSTRAK

Evolusi teknologi 5G untuk generasi seterusnya dalam aplikasi berkelajuan tinggi memerlukan dorongan inovasi yang ketara bagi membangunkan sistem komunikasi tanpa wayar. Disertasi ini bertujuan untuk menangani cabaran berkaitan kelajuan tinggi serta mengatasi tarik-ulur bagi meningkatkan prestasi liputan bagi penerima 5G New Radio jalur C. Kajian ini memperkenalkan sistem penerima jalur lebar 5G New Radio dengan Tahap Merit (FoM) yang tinggi, direka khas untuk aplikasi jalur C sub-6 GHz dan dilaksanakan melalui proses CMOS Silterra 130 nm. Sistem penerima ini menggabungkan konfigurasi Penguat Hingar Rendah (LNA) dua peringkat untuk mencapai gandaan yang tinggi dalam lebar jalur sasaran 3 hingga 5 GHz, tanpa mengorbankan kelinearan, angka hingar (NF), dan kestabilan. LNA ini diintegrasikan dengan litar penjana IQ inovatif bagi memastikan penjanaan RF quadrature pada empat fasa: 0° , 180° , 90° , dan 270° . Pencampur keseimbangan berganda, yang diintegrasikan dengan litar penjana IQ, disokong oleh 3 hingga 5 GHz VCO hibrid untuk membentuk isyarat perantaraan (IF) I dan Q dalam julat 100-200 MHz, yang seterusnya dipertingkatkan dengan peringkat Penguat Transimpedance (TIA) bertindan. Hasilnya, sistem penerima mencapai parameter utama dengan gandaan 35.6 dB, kelinearan 16.1 dBm, dan angka hingar (NF) 4.2 dB pada penggunaan kuasa hanya 12 mW. Prestasi VCO menunjukkan tahap hingar -120 dBc/Hz isyarat keluaran sehingga 8 dBm. Oleh itu, sistem penerima yang dicadangkan mencapai tahap merit (FoM) tinggi sekitar 94 dB, serta menunjukkan kepelbagaian dan kebolehpercayaan yang tinggi untuk sistem 5G New Radio.

HIGH FIGURE OF MERIT (FOM) VERSATILE 5G C BAND NEW RADIO IQ RECEIVER SYSTEM

ABSTRACT

The evolution of 5G technology for the upcoming generation of high-speed applications demands a substantial drive for innovation to develop a more extensive wireless communication system. This dissertation aims to address the challenges associated with high speeds and overcome trade-offs to enhance coverage performance for the 5G New Radio C Band receiver. It introduces a high Figure of Merit (FoM) 5G New Radio wideband receiver system, designed for sub-6 GHz C band applications and implemented using the 130 nm CMOS Silterra process. The receiver system incorporates a dual-stage Low Noise Amplifier (LNA) configuration to achieve a high and consistent gain across the target bandwidth of 3 to 5 GHz, without sacrificing linearity, noise figure, and stability. The LNAs are integrated with an innovative IQ generator circuit to ensure RF quadrature generation at four phases: 0° , 180° , 90° , and 270° . The double balance mixer, integrated with the IQ generator circuit, is supported by 3 to 5 GHz free-running tailless hybrid VCOs to form I and Q Intermediate Frequency (IF) of 100-200MHz, further enhanced with stacked Transimpedance Amplifier (TIA) stages. Consequently, the entire proposed receiver system achieves key parameters of 35.6 dB gain, linearity of 16.1 dBm, and a noise figure (NF) of 4.2 dB under 12mW power consumption. The VCO's phase noise reaches -120 dBc/Hz with output signal power up to 8 dBm. Therefore, the proposed receiver system offers a promising solution for achieving a high FoM around 94 dB, demonstrating high versatility and reliability for the 5G New Radio system.

CHAPTER 1

INTRODUCTION

1.1 Research Background

5G embodies the breadth and enormous depth of innovative and comprehensive mobile wireless communications technology. The future of 5G is audacious [1]. It is far more than the next generation of the mobile networks. The trend of the technology such as cloud computing, artificial intelligence (AI) and machine learning (ML) augmented reality (AR), virtual reality (VR) and billions of connected devices are heading towards higher and newer heights [2]. The 5G interconnected network technology shown in Figure 1.1 assure faster, more reliable and near –instant connections that connecting people and things everywhere. The enhancement of the 5G accommodates everyone to feel a real time live events and video streaming, thus enhancing communication especially in some urban areas.



Figure 1.1 5G interconnected network [1]

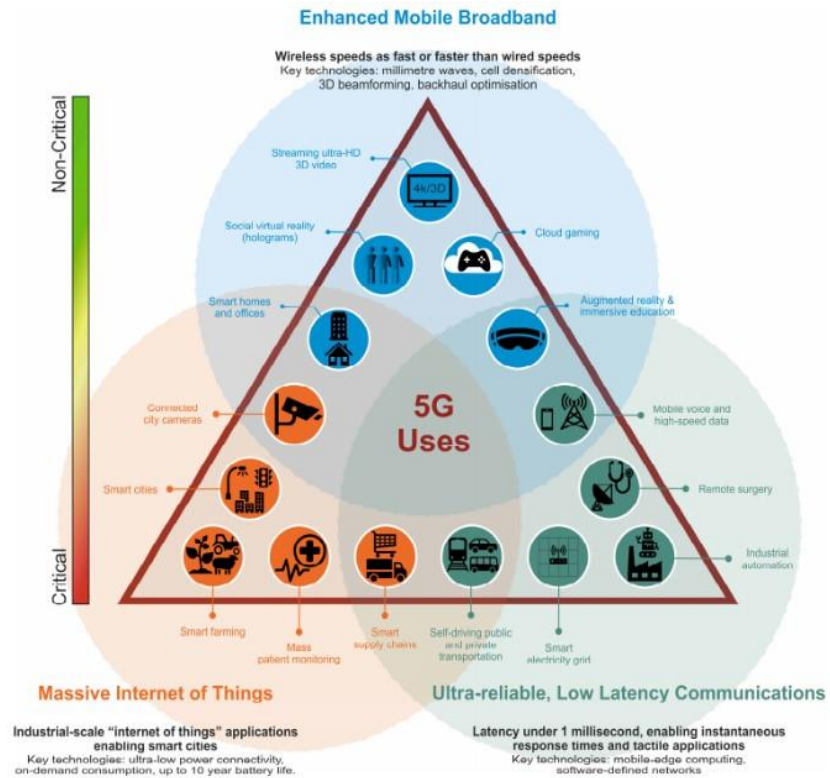


Figure 1.2 5G cases landscape [3]

The smart devices with AI feature create more customised and personalised environment for everyone. There would be three cases for the 5G functionality as shown in Figure 1.2 firstly would be an enhanced mobile broadband (eMBB). This refers to the target of the 5G peak and average data rates, capacity and coverage as compared to the conventional type of the mobile broadband. The eMBB specifies a 5G design capable of supporting up to 20 gigabits per second (Gbps) in the downlink (DL) and 10 Gbps in the uplink (UL). Secondly, would be a massive machine type communications (mMTC) which supports the 5G IoT use cases with billions of connected devices and sensors. It covers both low-data rate or low bandwidth devices with infrequent bursts of data requiring long battery life as well as very high bandwidth and high data rate devices. Thirdly would be an ultra-reliable and low latency communication (URLLC) which focuses on the applications that require fail-safe, real-time communications

example as autonomous vehicles, the industrial internet, smart grids, infrastructure protection and intelligent transportation system. This would be a paramount consideration whereby it can accommodate low facilities in a highly populated area, thus transforming into a truly connected world [4].

As the advancement with time, the fourth generation (4G) technology shows intrinsic limits and no longer sufficient to support the requirement and the need of emerging technology which require lower latency and higher traffic capacity [5]. Thus, this leads the Third Generation Partnership Project (3GPP) to set and develop a new standard for the communication need since 2015. The 3rd Generation Partnership Project (3GPP) is an industry consortium responsible for developing the standards for mobile telecommunications including the protocols, architectures, system requirements and so on. Release 15 a.k.a Rel -15 of the 5G NR specification is the first implementable standard for the 5G and it established a flexible foundation to facilitate the future release of 5G features [2] –[6]. This next big thing is known as New Radio (NR). NR is the new standard for wireless communication and foundation for the 5th generation of mobile networks. It is expected that 5G network will be the predominant option for communication industry in 2020 and following decade. NR are design to meet the criteria and performance laid down by International Telecommunication Union (ITU) for International Mobile Telecommunications for 2020 (IMT-2020) [7].

The potential of 5G is significantly greater than that of its forerunners where some of the new applications enabled would be multi-gigabit wireless mobile broadband, fixed broadband wireless access, augmented reality (AR) and virtually reality (VR), autonomous vehicles, vehicle to everything (V2X) communications, the mobile internet of things (IoT) and wireless industrial IoT(IIoT). The Long-Term Evolution (LTE) is to 4G as NR is to 5G. The 5G NR standard is still being developed to support the increased

dependability, more flexible networks, faster data rates, better coverage, and lower latency [1].

1.2 Receiver for 5 G Applications

The state-of-the-art 5G technology is a rapidly evolving landscape, with advancements in network infrastructure, edge computing, and integration into various platforms. There are many semiconductors' companies moving towards the development and the deployment of 5G solutions [8]. Narrowing the scope in the 5G platform, which is the receiver for 5G applications symbolizes one of the critical components in the 5G network infrastructure. They operate across the frequency bands inclusive of sub 6 GHz and mmWave and are typically integrated into smartphone, IoT devices and 5G base stations [9] - [10]. There are essential key components and technologies indulged in which are through an antenna array of massive MIMO to increase the signal quality and alleviate the interferences. Next, the front end of RF blocks involved would be LNA, filters, mixers and duplexers which are responsible to process the signal to ensure sufficient output signal. These signals need to be processed in the baseband processing to perform decoding and signal reconstruction tasks to be further managed by the power management systems.

1.3 Receiver for 5 G C Band applications and design specs

The 5G C Band typically refers to the mid band frequency in the range of 3.3 GHz to 4.2 GHz spectrum whereby it is crucial for 5G networks. This band is used for 5G networks, providing a good balance between coverage and capacity [11]. The modulation schemes which are commonly used are QPSK, 16QAM, 64 QAM and 256 QAM and besides the channel bandwidth is up to 100MHz per channel with the possibility of carrier aggregation to achieve higher bandwidths. Furthermore, the

estimation receiver's noise figure should be below 6 dB and the gain should be higher than 20 dB . The general application which emulates the specification of the 5G C band receiver is mobile devices, base station, smart cities, industrial IoT(IIoT) and many more. This band is particularly significant for 5G deployments as it offers a good mix of speed and range making it useful for the wide range of use cases[12]. The eMBB is one of the primary use cases for 5G C band which able to provide high -speed internet access supporting streaming HD and 4K videos, Virtual Reality (VR) and Augmented Reality (AR) experiences. Besides that, the demand for the 5G C Band is high especially during the Covid-19 pandemic as it helps to facilitate high speed internet to homes and businesses where fibre optic infrastructures are not feasible such as broadband internet services, remote work and education. Moreover, 5G C band also supports the smart homes in smart cities [13].

1.3.1 The challenges in Meeting 5G C Band

As the demand becomes higher in terms of performance, bandwidth and efficiency to meet the standards of 5G C Band systems, it also introduces technical challenges to meet the high data rates, low latency and reliable connections as shown in Figure 1.3. Firstly, the primary challenges in designing a 5G C Band receiver is supporting for the wide channel bandwidths up to 100 MHz per carrier with multiple carriers. This demands high linearity, low noise figures and efficient signal processing to handle wideband signals without signal distortion. As the C Band spectrum is densely packed, the receivers must ensure better sharp and high-quality filter system to filter out the interferences from the neighboring channels and coexisting systems ensuring minimal insertion loss especially under the high frequencies and wide bandwidth

platform. Next challenge is the power efficiency and cost to support the receiver system with the minimal usage of battery power and with a cheaper cost of manufacturing. Furthermore, under larger bandwidth in 5G C Band, it is difficult to maintain signal consistency that could also lead to an increase in phase noise and causes fast signal variation in the time domain and higher variation in the power domain. Besides that, the modern 5G C Band receivers face difficulty during integration while meeting performance specifications, especially dealing with the risk of parasitic, interference and heat dissipation issues. Therefore, meeting the 5G C Band receivers [14] demand, involves the performance balancing, power efficiency, size and cost while addressing interference, bandwidth and regulatory constraints. Besides the technological advancements in materials, integration and digital processing, creative mitigation techniques are also crucial in overcoming these challenges and to achieving better standards required for the 5G C Band receiver networks.

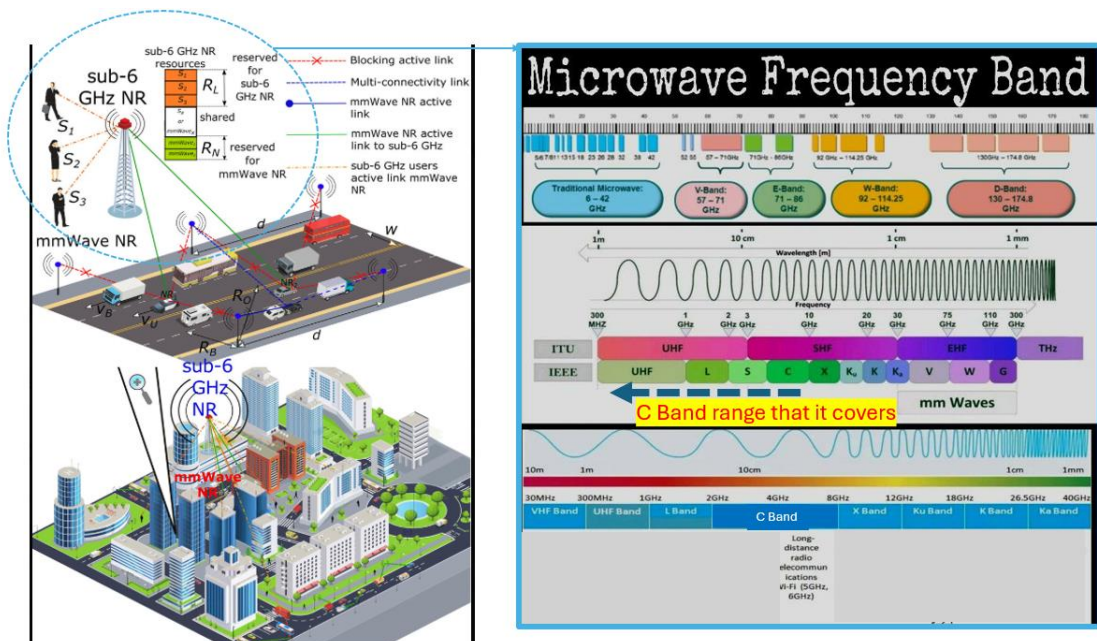


Figure 1.3 Sub 6 GHz NR Receiver for C Band range [14]

1.3.2 The challenges in 5G Band, which narrows towards sub 6 GHz New Radio GHz.

While 5G offers exciting possibilities, it also faces several challenges in mmWave that influence the focus towards sub 6 GHz frequencies. Firstly, limited coverage, where mmWave signals possess shorter wavelengths, which result in a reduced coverage area and a higher susceptibility to being obstructed by physical barriers such as buildings, foliage, and precipitation. These characteristics necessitate a more densely deployed network infrastructure, which can lead to increased costs [4].

Millimeter-wave (mmWave) frequencies are typically defined as those within the 30 GHz to 300 GHz range, which corresponds to wavelengths between 10 millimeters (1 centimeter) and 1 millimeter [9]. Due to their shorter wavelengths, mmWave signals do not travel as far as lower-frequency signals before they attenuate or weaken. Additionally, these signals have a harder time penetrating materials, making them more prone to absorption and reflection by obstacles encountered in urban and natural environments [15]- [20]. The higher frequency of mmWave signals also means that they can carry more data, which is beneficial for high-bandwidth applications [21].

However, the trade-off is that to maintain a robust and reliable mmWave network, service providers need to install more base stations or small cells at closer intervals compared to networks operating at lower frequencies. This denser network infrastructure is necessary to ensure that the signal can reach users without significant degradation, especially in areas with many physical obstructions. The requirement for a denser deployment translates into higher costs for network providers. More base stations mean more equipment, more installation labor, and potentially more site rentals, which all contribute to the overall expense of building and maintaining a mmWave network. In summary, while mmWave technology offers the potential for high-speed

wireless communications, its deployment is challenged by the physical limitations of the signal propagation and the economic implications of constructing a dense network infrastructure.

Moreover, the devices that incorporate mmWave technology typically necessitate specialized antennas and components, which at present, result in higher costs when compared to devices that operate on sub-6 GHz frequencies [22]. Furthermore, higher device cost of the devices acts as a barrier to their widespread use, which in turn affects the entire network ecosystem and the potential benefits. In a nutshell, the sub -6 GHz NR receiver system would be the suitable band application compared to mmWave especially due to the lower cost. It is an essential application to meet with 5G coverage, due to its mobility and efficiency, to be able to balance speed and range. It serves as the foundation of widespread 5G deployment, ensuring reliable connectivity while handling interference, multi-user scenarios and spectrum sharing.

1.3.2(a) The advantages of Sub 6 GHz.

There are important advantages of Sub 6 GHz which is, they have the capability to cover wider areas and penetrate obstacles more effectively. This results in more extensive network coverage, which is particularly beneficial in regions that are not densely populated, such as rural and non-urban areas. Lower frequency signals, such as those in the sub-6 GHz range, have longer wavelengths [23]-[24]. These longer wavelengths are less susceptible to attenuation caused by obstacles like buildings and trees. Consequently, they can travel greater distances without significant loss of signal strength and this characteristic makes sub-6 GHz bands well-suited for providing coverage over large geographic areas, which is why they are often used for cellular networks that need to serve both urban and rural locations. In contrast, higher frequency signals, such as those used in millimeter-wave (mmWave) bands, have shorter

wavelengths and are more prone to attenuation. While they can offer higher data rates due to their larger bandwidth, their range is much shorter, and they struggle with penetrating materials, making them more suitable for dense urban environments where small cells can be deployed closely together [25].

Next is deploying sub-6 GHz technology can be more cost-effective than establishing entirely new millimeter-wave (mmWave) networks because it allows for the use of existing infrastructure and technologies. This approach can reduce the need for significant capital investment in new hardware and facilities, as sub-6 GHz deployments can often utilize current cellular towers, backhaul connections, and other network components [26].

Sub-6 GHz frequencies have been a backbone of wireless communication for many years, and the equipment supporting these frequencies is widely deployed. This existing network infrastructure can be upgraded or augmented to support new sub-6 GHz services, such as 5G, without the need for a complete overhaul [27]. In contrast, mmWave networks operate at much higher frequencies and require a denser network of cell sites due to their shorter range and poorer penetration through obstacles. Building out a new mmWave network would involve significant investment in new cell sites, backhaul infrastructure, and other network elements, which can be costly and time-consuming [4]. Moreover, sub-6 GHz networks can cover larger geographic areas with fewer cell sites compared to mmWave networks, leading to more efficient use of resources and potentially faster deployment times. This efficiency is particularly beneficial in rural or suburban areas where the deployment of a dense network of mmWave cell sites may not be economically feasible.

Next, is faster adoption where lower-cost sub-6 GHz devices facilitate broader adoption among users, which in turn contributes to an expanded user base and

accelerates the expansion of the 5G network ecosystem. In summary, leveraging existing infrastructure for sub-6 GHz deployments can lead to cost savings, quicker deployment, and a more efficient use of resources compared to the construction of new mmWave networks.

1.3.2(b) The approach towards Sub 6 GHz.

The difficulties encountered have prompted a strategic pivot towards prioritizing sub-6 GHz frequencies shown in Figure 1.4 resemble the initial deployment of 5G networks in numerous areas. Although millimeter-wave (mmWave) technology delivers exceptional speed and capacity for specific scenarios such as densely populated urban centers, the broader coverage, reduced costs, and quicker implementation possibilities of sub-6 GHz frequencies render it a more practical option for widespread 5G network adoption. Firstly, balance approach where numerous service providers are adopting a dual-pronged strategy, leveraging sub 6 GHz frequencies to achieve broad coverage and millimeter-wave (mmWave) technology for high-speed applications in specific areas. Secondly, the priority of Sub 6 GHz which allows broader 5G access initially and then gradual integration of mmWave as technology matures and costs decreases. Globally, the sub-6 GHz spectrum is the primary frequency band utilized for the deployment of 5G networks. This band offers extensive coverage and the capacity to serve many users. On the other hand, mmWave deployments are less common but are expanding in certain areas and for specific applications. Continuous research and development efforts are focused on enhancing both sub-6 GHz and mmWave technologies to achieve broader coverage, increased data transmission speeds, and improved cost-effectiveness.

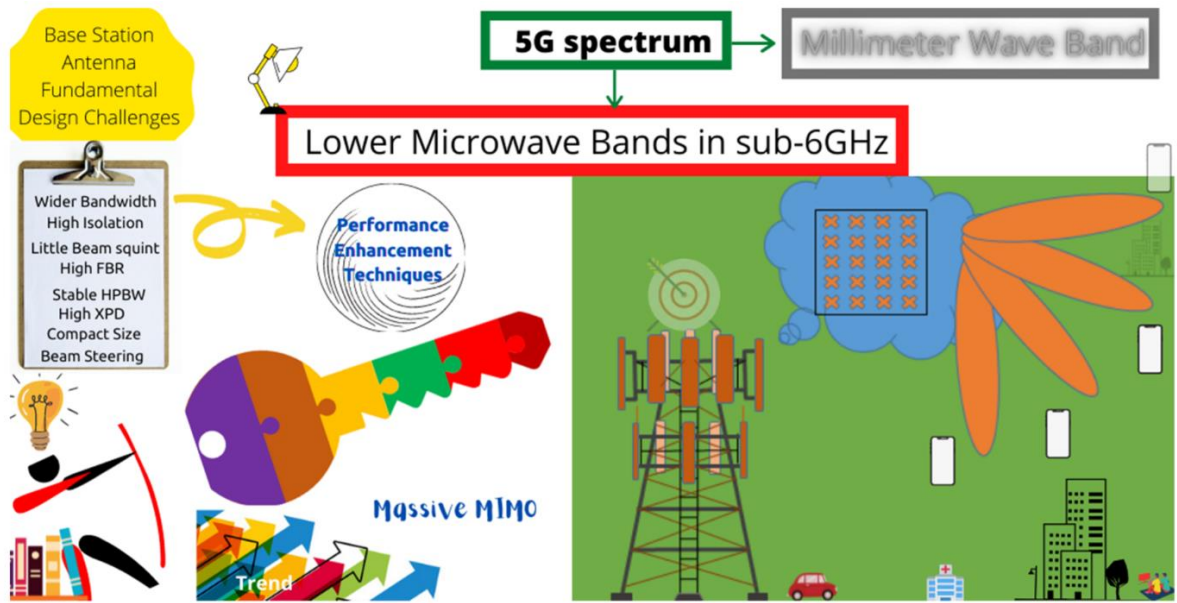


Figure 1.4 The feature towards enhancing sub 6 GHz [16]

Real 5G is combination of sub 6 and millimeter wave happening is a global scale. Higher frequency signals can transmit more data, which translates to more bandwidth and rapid network speeds as shown in Figure 1.5. Therefore, at a certain extent, mmWave 5G devices can facilitate maximum speeds of around 4-5Gbps, even though the customer speeds are often lower. MmWave can be faster than the most wired fiber broadband connections, by comparison, the best sub-6GHz network can hit a few hundred Mbps, even though tens of Mbps is more realistic. However, the drawback of the mmWave signals is that they are more susceptible to losses when passing through obstacles. There are only few hundred megabits per second are visible unless a direct line of sight with the mmWave cell tower. In such where the lower frequency of 5G bands come into the picture and these lie in the range of 1 to 6 GHz and referred to as sub-6 GHz 5G.

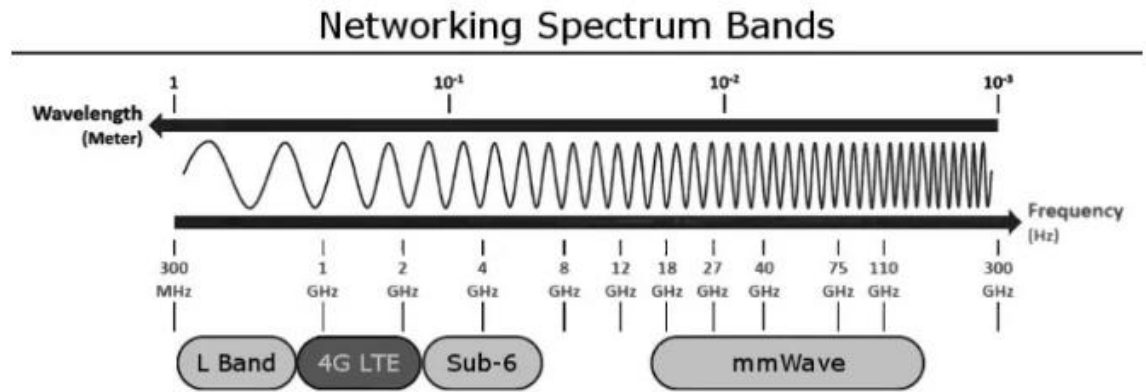


Figure 1.5 Network Spectrum Bands of 5G

The sub-6 GHz 5G bands cover similar frequency ranges as the previous generations and not as departure as mmWave 5G, which offer slight improvement in terms of the speed over LTE , more bandwidth and faster user speeds. This includes the ability to penetrate obstacles. The sub-6GHz spectrum is known to be as a backbone of the global 5G deployments.

Therefore, the mobile communications in the 5G deployments supports only sub-6GHz even though it consists of millimeter wave spectrum and the fastest way to get the devices wanted is through the sub-6Hz only. The support towards the sub-6GHz is extensive due to the higher cost bearing required in the millimeter wave. Therefore, the ABI Research forecast that approximately 90 percent of 5G cell sites emerging markets will be operating with the support for a combination of the sub-6GHz bands by the year 2026.

The sub6 GHz band provide the optimum coverage and it is faster that the 4G which has a longer range and more affordable for carriers to implement. While millimeter wave (mmWave) with its large amount of bandwidth able to meet at a very high-capacity demand. However, its poor propagation and cost of deployment shift it in disadvantage condition to sub -6GHz for 5G deployment. The sub 6 Ghz able to meet

the sufficient capacity and its higher propagation over a wide distance and not attenuated by the rain.

Furthermore, most of the handset vendors focused on the emerging technology of the sub6-GHz bands where it gives an additional benefit of keeping the bill of the material cost down. The 5G handset shipments supporting the sub-6Ghz band will be expected to expand to nearly 600 million by 2026 at a Compound Annual Growth Rate (CAGR) of 22.7 percent from 2020 [28]. It is deemed an importance towards sub-6GHz in supporting the key applications such as the Internet of Things (IoT) as well as the Fixed Wireless Access (FWA). However, these applications require very robust propagation characteristics and sufficient capacity capability which can be supported and provided by the sub-6Ghz bands. Therefore, for applications such as LTE and sub 6 GHz technologies the performance especially on the low power receivers are critical. The specifications ensure that the receivers can handle the required frequency ranges within gain balance, interference tolerance and minimum pulse width response, among other factors.

1.3.3 Low Power Receiver

Past few years, it would be changing 1 billion of batteries per day to maintain the network of devices. Due to the higher impact of the battery disposal at higher scale, nobody seems to take care of the battery maintenance issue whereby it limits the mass adoption of 5G solutions [29]. Thanks to the 5G solutions today, most devices in the world today, operates on a battery that provides longevity for an average of three years. It seems very generous considering of today's technology that have batteries with shorter lives. There are few specifications for the receiver performance needed to consider which the power, sensitivity, data rate is and signal to interference ratio (SIR)

and the adjacent channel rejection. Generally, there has been trade-off among one another, however figure of merits captures its relative impact across all types of receiver's frequencies, modulations and so on.

Several receiver architectures especially, the ultra-low power receiver supports the variation of a passive envelope detection radio frequency (RF) front end, reducing the power-hungry RF blocks such as the low noise amplifiers (LNAs) and RF local oscillators (LOs). There are some architectures are not considered as ULP, like hybrid architectures added back the LNA block for the sensitivity improvement with the integration of the passive mixer incorporating some RF blocks. These architectures somehow dissipate power $> 20\mu\text{W}$ and $>100\mu\text{W}$ as well [30]-[31].

On the other hand, passive transformers and matching networks integrated at the front of the envelope detector (ED) to eliminate the noise bandwidth and improve the sensitivity up to 20dB, thus extending the wireless range. This passive voltage booster performs better with its higher RF ED input impedance which would be easier to achieve especially at the lower frequencies $< 10\text{nW}$ receivers which tend to be sub gigahertz. However, the passive envelop detector that is used for the down conversion posses with a wide bandwidth but encounter higher noise which limits the sensitivity at around -50dB referenced to 1mW. The baseband gain and filtering stage operate in the sub threshold with a minimum bandwidth to lower the power typically achieving a minimum voltage in 1-10mW range. The data rates of these receivers are less than 1kb/s however limited by its speed and bandwidth of the subthreshold analog and digital baseband circuits [32].

1.4 Challenges and Trade-Offs in the Sub 6 GHz Receiver system

The sub 6 GHz frequency bands are widely used for various communication systems, including mobile networks and are critical for 4G/LTE and 5G technologies [30]. A receiver system operating in the sub 6 GHz range faces the gain imbalance were ensuring that the gain imbalance is less than 1 dB which is crucial and important to maintain the signal integrity [31].

Next would be the antenna design which must be optimized for the sub 6 GHz spectrum to ensure efficient signal reception. The dimensions and specifications of the antenna play a crucial role in the receiver's performance.

Thirdly, noise figure where at low noise figures are necessary to minimize the signal degradation and improve the receiver sensitivity.

Fourthly, in terms of the linearity, the receiver must maintain the linearity over the operating frequency to avoid distortion of the signals received.

Next, Sub 6 GHz bands congested with various signals from WiFi, LTE and other sources [32]. Designing selective filters to extract the desired signal while suppressing unwanted ones is crucial. Balancing sensitivity, filtering, and processing power with limited batter life in mobile devices is a constant challenge [33]. Due to mobility and environmental factors, sub 6 GHz channels experience rapid changes, requiring the receiver to continuously estimate and adapt to maintain optimal performance. Even small timing errors can significantly impact data recovery. Achieving accurate synchronization in the presence of multipath and interference is crucial.

1.5 Problem Statement

With the advancement of the Sub 6 GHz receiver, there are recent problems and several challenges that are continuously being addressed. The Sub-6 GHz frequency bands are densely populated with a variety of signals from technologies such as LTE, Wi-Fi, and other forms of wireless communication. This congestion necessitates that receivers in the Sub 6 GHz band encounter a stringent requirement to satisfy and improve the efficiency of the system. Firstly, the challenges would be compromising the performances by mitigating the tradeoffs of gain, linearity, noise figure (NF) and power consumption of the receiver system especially for the respective blocks of Low Noise Amplifier (LNA), Mixer and Voltage Controlled Oscillator (VCO) [5]-[13], [34]-[43].

Firstly, as the LNA which is the front-end stage of the receiver, adopted multiple techniques to ensure the essential performances are met. Despite many proposed techniques applied e.g. as forward-body bias technique applied in [41] which can reduce power consumption and improve the noise factor of the LNA, but the linearity tends to degrade. Another topology of folded cascoded LNA proposed to ensure high gain but exists a tradeoff between power consumption and gain [42]. The approach towards a higher bandwidth with low power consumption is challenging, which limits the signal amplitude and quality and affects the SNR with low gain and high noise. [33]. In addition, in certain cases, especially dealing with multiple levels of interferences, especially under the wideband implementation which affects the signal in the sub-6 GHz frequencies, and it tends to diminish more over time and distance which is difficult to detect weaker signal in particularly at the areas under limited coverage or within challenging environments [36]. All these customized architectures and methods focus on improving and satisfying a specific parameter, indirectly impacting the other critical

performances and introduces more difficult tradeoff to solve which is linearity, noise and gain tradeoffs under especially with the requirement of low power and wide bandwidth.

This is followed by the next stage of the LNA's building block which is the down-conversion mixer. In recent works, the IQ down conversion mixer encounter I and Q mismatches that result in poor image – rejection ratio vulnerable to the system. Poor image rejection is known to be sensitive and that would cause mismatches in the receiver path [13]. Some complex IF mixer in the receiver relies on through calibration mechanism but it is difficult to maintain the I and Q in sub 6 GHz bandwidth. Furthermore, additional effort on design may impact on additional complexity and it is not recommended for area reduction plan and adding extra cost. On the other hand, intermodulation and unwanted harmonics are significant especially dealing with complex mixer with mixed signal simulation. These harmonics introduce into the mixer degrade the signal integrity which results in poor signal-to-noise ratio (SNR). In fact, with poor isolation between these ports lead to signal and power leakage and crosstalk which limits the signal quality and affects the entire mixer functionality [17]-[18], [37] – [43].

Consequently, during the mixer's operation, the carrier signal needed to down convert the signal in the mixer with the help from the signal from VCO which actively providing the carrier signal. Therefore, maintaining purity and quality is utmost important. In many reported works, ensuring the low phase noise with high output signal power under low power consumption has been a tough challenge. Work in [15] able to achieve a very low phase noise performance at 1MHz offset but with the expense of additional power needed. Phase noise and low power has been an inevitable trade off and adjusting the power consumption which is not a preferable method just to realize a

low phase noise performance [15]. Besides that, another challenging design trend for CMOS VCO is to achieve a low phase noise across a wide frequency range. To tackle the bandwidth limitation of the VCO, the most commonly are used switched capacitor banks for frequency tuning, and in fact some works [18] used a digitally controlled varactor arrays, but however it contributed to major portion of resistance parasitics to the oscillation resonant tank which eventually degrades the phase noise and tuning range. In conjunction to tuning range, it is hard to achieve a high figure of merit as well, which resulted in high power consumption that can be even up to 200mW [43]. In some cases, the stability in tuning frequency is not linear for the VCO wideband tuning. Therefore, to achieve a stable and accurate oscillation frequency over process, voltage and temperature variation (PVT) is taxing which requires an additional circuit to control the loop and with several compensation mechanisms [43]. Moreover, in the IQ receiver system, the area of the VCO especially in generating for a wideband range requires high passive tank contributor and thus this would increase the cost as well for the entire receiver size [44].

The receiver in the integrated system directly impacts on the entire system power consumption, system linearity, entire noise, gain and stability performance. In the IQ receiver system, many researchers developed the IQ imbalance compensation methodology using an IQ demodulator which is then filtered and amplified [13]. Besides that, works using digital implementations, the direct analog frequency down conversion encounter two side effects that can be observed in the spectrum of received signal which is the DC offsets, and the sideband image effects. The DC offsets limit the dynamic range of the receiver and cause interferences that affect the fundamental signal quality [45]. Considering all important criteria, the significant concern of the system performance is the figure of merit of the system performance. The figure of merit which

resembles a performance measurement that quantifies the efficiency and effectiveness of the receiver system which includes the sensitivity, noise figure, gain and other paramount performance metrics. The longevity of the receiver is also dependable to the versatility of a receiver to be suitable and efficient.

The sustainability and efficiency of the entire receiver to operate for a long-term run can be only achieved when the solution to mitigate all these challenges are critically addressed and executed with techniques. This is a significant concern because excessive degradation of the sub blocks performance in the integrated system may also affects the power usage which not only shortens the battery life of the devices but also impacts the sustainability of the entire network infrastructure [40]. It is also imperative to focus on optimizing the design of receivers to enhance their energy efficiency. By doing so, it can extend the battery life of mobile devices, which is a critical factor for users who rely on their devices throughout the day [41] – [46]. Therefore, the focus on this research is to achieve, solve and mitigate the trade-offs of the standalone performance of the LNA , mixer and VCO with better performance across the sub 6 GHz bandwidth which is from 3 to 5 GHz range. Moreover, the ultimate target to ensure an overall high figure of merit (FoM) of the receiver system with enhanced performance of these front-end blocks, managed to solve all the trade-offs and acquire a versatile receiver architecture that meets the sub 6 GHz receiver requirements and target specifications

1.6 Research Objectives

By understanding and addressing these challenges and problems of the sub 6 GHz, ideas evolved to mitigate all challenges through various advancements to optimize the receiver design. The research objectives are as follows:

- I. Design the standalone LNA, mixer and VCO and integrated them together as CMOS receiver achieving an overall low power less than 20mW, low noise figure, NF with higher port to port isolation and with minimum I and Q quadrature phase error at the receiver's output to be less than 4 dB.
- II. Design and verify the results of the pre-layout, post-layout and measured results of the proposed 5G Sub 6 GHz receiver until target specification are met.
- III. Validate the fabricated receiver's functionality to meet the sub 6 GHz standard and owned its versatility as an efficient and reliable high FoM receiver of above 90 dB.

1.7 Thesis Scope

The scope of this project elaborates on the design of the high figure of merit (FoM) versatile Sub 6 GHz C band receiver in low cost 130nm Silterra CMOS technology. The construction of the receiver is built in stages starting from the prelayout, postlayout and towards the measurement which is done in detail for the architecture of the receiver starting from the front end wideband low noise amplifier (LNA) followed by the development of the I and Q quadrature generation integrated with the mixer and next with the hybrid structure of the VCO. The design build up is fulfilled with the aid of the software tools which is the Electronic Design Automation (EDA) tool in the Cadence. This tool is the most significant in the semiconductor integrated circuit (IC) design to ensure reliability and to test the design correctness under varying conditions. In this platform, Cadence Virtuoso facilitates the design development and simulation using Cadence Spectre from the top to down approach of

the schematic to post layout and able to accelerate the whole design process verification with extensive optimisation of the receiver design until reaching the target specification. The fabrication process would be conducted and completed by the semiconductor Silterra foundry using the EDA tools where the final top level of the receiver integration with the Silterra generated metal filling and is streamed out from the Cadence as GDSII file and sent to the foundry to start for the fabrication process. Once the chip has arrived, the measurement process would be carried out in the Collaborative Microelectronic Design Excellence Center (CEDEC) lab at the USains, USM to ensure, validate and verify the entire receiver performances on wafer. The on-wafer measurement using probe station equipped with Vector Network Analyzer (VNA), Spectrum Analyzer (SA), Noise Figure Analyzer (NFA), Signal Generator to measure the S-parameters, Output powers, Noise Figures, 3rd order Intercept Point (OIP3) respectively for the receiver and whereas the Parameter Analyzer to supply the DC voltage and ground supply. The Signal Source Analyzer (SSA) is used to measure the phase noise of the VCO and oscilloscope to measure the signal quality, output and input power of the proposed receiver. Therefore, the whole plan to build up the whole receiver architecture is applied to certify the novel proposed receiver as a versatile 5G Sub 6 GHz C Band receiver that can meet the standard needed.

1.8 Thesis Organization

The thesis is divided into 5 Chapters which are organized as follows:

Chapter 2 introduces the literature reviews and general background on the detailed works on different types of on various latest published work and techniques adopted on each LNA, Mixers, VCOs and entire Receivers. Furthermore, table of comparison of each block and entire receiver was included and concluded.

Chapter 3 introduces the design methodology of the proposed Receiver, explaining with the detailed mathematical analysis for each subsequent blocks of the LNA, Mixer and VCO and as whole Receiver system and testbench setup used for each of the blocks and entire receiver for pre-lay, post-lay and measurement.

Chapter 4 presents the results of pre-schematic simulation, to post layouts and finally to measurement results. In addition, the comparison between each of the results were included with the comparison of recent reported works and the proposed design with its fabricated chip micrograph are described as well.

Finally, Chapter 5, shows the discussion and conclusion of the proposed research along with its improvements and possibilities that would be suggested for future work.

CHAPTER 2

LITERATURE REVIEW

2.1 Introduction

In some communication system, data transmission only occurs in one direction. Simplex transmission is one of the signal direction systems which performs data transmission in one direction only. But Simplex transmission is not often used as the receiver which is unable to feedback any errors or control signals to the transmit end. In modern communication systems, system transmission must carry in two -way interchangeable data and information transfer. Both ends of the radio channel need to integrate the transmitting and receiving capabilities to achieve two-way communication system. The function of a wireless transmitter is to transmit a frequency waveform encoded with information signals while wireless receiver is to detect and receive incoming modulated signals. A device comprising both transmitter and receiver which combines and shares common circuitry is known as transceiver.

The quality of wireless transmission performance is influenced by more than just the channel through which it propagates, and it is also contingent upon the capabilities of the transmitting and receiving equipment. Therefore, the architecture selected for the implementation reveals in an important notation of performance such as power dissipation, complexity, and production cost. Additionally, selectivity and sensitivity requirements are equally important in RF front-end receiver [14]. Receiver sensitivity refers to the lowest strength of an incoming signal that a receiver can detect to achieve a specified signal-to-noise ratio (SNR) at its output. This is a critical parameter as it determines the minimum signal level at which the receiver can operate effectively.

Receiver selectivity, on the other hand, is the ability of a receiver to discern and process the desired signal while ignoring other signals that are close in frequency. This characteristic is essential for the receiver to function properly in an environment where multiple signals may be present. Wi-Fi or LTE can be affected by noise from platform components, which can lead to a degraded SNR at the radio receiver's input. This degradation can impact data throughput and the range of the wireless link. Generally, there are unwanted interferences present close to the spectrum of the desired signal that will corrupt the demodulation in the receiver system. Therefore, filters are required to eliminate the effects of these interferences. The overview of LNA, Mixer and VCO that develop the Sub 6 GHz would be briefly explained in this chapter.

2.2 LNA Overview

Section 2.2 focuses on LNA introduction, and its analysing and interpreting existing knowledge that is pertinent to this work. It establishes the foundation for this study, which is the primary focus of this thesis's investigation. The parameters used to analyse the performance of an LNA is discussed in Section 2.2.1. Then, in Section 2.2.2 explains on the various cascoded LNA and wideband LNA topologies which will be discussed, along with their related work summary shown in section 2.2.3. The literature review is necessary to demonstrate the significance of this research compared to previous studies.

2.2.1 LNA Performance Parameters

This segment discusses critical performance parameters for determining the effectiveness of an LNA. The performance of an LNA is measured by its gain, noise figure, power consumption, input impedance matching, and linearity. A trade-off between these parameters must be made to get the optimum result.